NIH Public Access
Author Manuscript
Transl Stroke Res. Author manuscript; available in PMC 2015 October 01.

Published in final edited form as:
Transl Stroke Res. 2014 October ; 5(5): 586–594. doi:10.1007/s12975-014-0353-y.

Deferoxamine attenuates acute hydrocephalus after traumatic brain injury in rats

Jinbing Zhao, MD, **Zhi Chen, MD**, **Guohua Xi, MD**, **Richard F. Keep, PhD**, and **Ya Hua, MD**
Department of Neurosurgery, University of Michigan, Ann Arbor, Michigan, USA

Abstract

Acute post-traumatic ventricular dilation and hydrocephalus are relatively frequent consequences of traumatic brain injury (TBI). Several recent studies have indicated that high iron level in brain may relate to hydrocephalus development after intracranial hemorrhage. However, the role of iron in the development of post-traumatic hydrocephalus is still unclear. This study was to determine whether or not iron has a role in hydrocephalus development after TBI. TBI was induced by lateral fluid-percussion in male Sprague-Dawley rats. Some rats had intraventricular injection of iron. Acute hydrocephalus was measured by magnetic resonance T2-weighted imaging and brain hemorrhage was determined by T2* gradient-echo sequence imaging and brain hemoglobin levels. The effect of deferoxamine on TBI-induced hydrocephalus was examined. TBI resulted in acute hydrocephalus at 24 hours (lateral ventricle volume: 24.1±3.0 vs. 9.9±0.2 mm^3 in sham group). Intraventricular injection of iron also caused hydrocephalus (25.7 ± 3.4 vs. 9.0 ± 0.6 mm^3 in saline group). Deferoxamine treatment attenuated TBI-induced hydrocephalus and heme oxygenase-1 upregulation. In conclusion, iron may contribute to acute hydrocephalus after TBI.

Keywords

Deferoxamine; hydrocephalus; lateral fluid percussion; traumatic brain injury

Introduction

Traumatic brain injury (TBI) is a leading cause of morbidity and mortality in children and adolescents (1). Each year in the United States, approximately 1.7 million people suffer a TBI (2). Ventricular dilation is a frequent phenomenon in TBI patients and may present in follow up exam and turn into post-traumatic hydrocephalus (PTH). Marmarou and colleagues reported that 44% of severe head injury survivors develop post-traumatic ventriculomegaly, among which about half of the survivors were classified as PTH (3). The incidence of PTH varies between studies from 0.7% to as high as 29% (4, 5). Post-traumatic hydrocephalus has been recognized as an indicator of worse outcome after TBI (6). However, the mechanisms of early and late ventricular dilation are still not well understood.

Correspondence and Reprint Requests: Ya Hua, M.D., R5018 Biomedical Science Research Building, University of Michigan, 109 Zina Pitcher Place, Ann Arbor, Michigan 48109-2200, U.S.A, Tel: 734-764-1207, yahua@umich.edu.

Conflict of Interest: Jinbing Zhao, Zhi Chen, Guohua Xi, Richard F. Keep and Ya Hua declare that they have no conflict of interest.

NIH-PA Author Manuscript
NIH-PA Author Manuscript
NIH-PA Author Manuscript

NIH-PA Author Manuscript

NIH-PA Author Manuscript

NIH-PA Author Manuscript

Intracranial bleeding is a common and serious consequence of TBI (7). MRI has shown a preponderance of hemorrhagic lesions compared to ischemic lesions during the acute phase after TBI. Thus, a study found that 56% of TBI patients had at least one intracranial bleed (8) and another showed that patients with greater initial total hemorrhagic contusion volume had more severe chronic brain atrophy (9). Our previous studies in intracerebral hemorrhage (ICH) revealed that iron released from hemoglobin contributed to brain edema, brain atrophy, and neurological deficits (10-12). Another recent study found periventricular iron accumulation with ventricular enlargement after intraventricular hemorrhage (IVH) (13). CSF iron levels are upregulated in 83% ICH patients (14), and they are increased as early as the first day in rat experimental ICH (15). Ten-fold higher CSF iron levels are detected in subarachnoid hemorrhage (SAH) patients, and a high concentration is maintained for the first 2 weeks after ictus (16). The deposition of iron in brain can be determined by specific staining and magnetic resonance imaging (MRI (17-19)).

Deferoxamine (DFX), an iron chelator, reduces brain injury in experimental TBI (20, 21), ICH (22, 23), IVH (24) and SAH (25). In this study, we investigated the role of iron and the effect of DFX in TBI-induced acute hydrocephalus.

Methods

Animal preparation and lateral fluid-percussion-induced traumatic brain injury models

Adult male Sprague-Dawley rats (280-320g) were purchased from Charles River Laboratories (MI, USA). All animal use protocols were approved by the University of Michigan Committee on the Use and Care of Animals. Rats were fasted, but with free access to water for at least two hours before surgery. Anesthesia was induced by 5% (v/v) isoflurane, and maintained by 2.5-3.0% isoflurane with a rodent mechanical ventilator (Tidal volume: 2-2.5 ml, respiratory rate: 55-60/min; Model 683, Harvard Apparatus, MA, USA). Rectal temperature was monitored and kept at 37.5 ± 0.2°C using a feedback-controlled heating pad. The right femoral artery was catheterized to monitor blood pressure and determine blood pH, PaO_2, $PaCO_2$, glucose and hematocrit.

Brain injury was induced using a fluid-percussion device (AmScien Instruments, Richmond, VA, USA (26, 27)). In brief, rats were positioned in a stereotactic frame (David Kopf Instruments, CA, USA) in a prone position. A longitudinal scalp incision was made along the midline to expose the bregma and lambda sutures. A right parietal craniotomy (5 mm in diameter, without dural laceration) was performed centered at 4 mm posterior and 3 mm lateral to bregma. A plastic female Luer-Loc hub was attached to the craniotomy site using cyanoacrylate adhesive followed by dental cement (3M ESPE Ketac Cem rediopaque, Germany) and linked to the fluid percussion instrument. After setting the desired pressure at 2.5-3.5 atm, and exact pressure for brain injury was recorded for each rat. After fluid percussion, the female Luer-Loc hub was removed, the skull flap fixed back with dental cement, and the scalp incision closed with 3-0 sutures. There was a temporary apnea after the fluid percussion and ventilation was maintained until recovery of spontaneous respiration. In a sham group, rats had the same procedures except the fluid percussion.

NIH-PA Author Manuscript

NIH-PA Author Manuscript

NIH-PA Author Manuscript

Intraventricular injection

Animal preparation was as described above. After positioning on the stereotactic frame, a longitudinal incision was made and a burr hole (1mm) was drilled on the skull. A 26-gauge needle was inserted directly into the right lateral ventricle (coordinates: 4.5mm ventral, 0.6mm posterior, and 1.6mm lateral to bregma) and 200μl of saline or $FeCl_3$ (0.5mmol/L) was infused (14μl/min) using a microinfusion pump (World Precision Instruments, FL, USA). The burr hole was covered by bone wax after injection.

Experimental groups

There were three parts in this study. First, rats undergoing a sham operation **(n=9)** or TBI (n=11) had an MRI and cerebrospinal fluid (CSF) collection via cisterna magna puncture at 24 hours after surgery. Brains were then perfused with PBS and used for hematoxylin and eosin staining, immunohistochemistry and brain hemoglobin concentration determination. In the second part, rats received an intraventricular injection of $FeCl_3$ (0.5 mmol/L, 200μl) or saline (n=5 for each group), and had an MRI scan after 24 hours. Third, rats were treated with vehicle (n=11) or DFX (**half-life about 3 hours,** 100mg/kg, intramuscular, n=13) at 2 and 14 hours after TBI. Brains were perfused after MRI examination and CSF collection at 24 hours after TBI for histology and immunohistochemistry.

MRI and lateral ventricular volume measurement

Under anesthesia with 2% isoflurane, rats were placed in a prone position and scans performed with a 7.0 T MR scanner (183 mm horizontal bore, Varian, CA, USA) as described previously (23, 24). T2-weighted and T2* gradient-echo sequence (GRE) scans were performed to evaluate lateral ventricular volume and lesion volume at 24 hours after TBI. Detailed parameters were: repetition time/echo time=4000/60ms or 250/5ms for T2 and T2* sequence respectively, field of view=35×35 mm, matrix=256×256, total slices=25, slice thickness=0.5 mm, slice gap=0, scan field: about 2 mm anterior and 8.6 mm posterior to bregma. Bilateral ventricles were outlined in T2-weighted images and measured using IMAGE-J software (version 1.45, NIH). Lateral ventricle volume was obtained by multiplying areas in all slices by slice thickness. Lesion volume was obtained in T2* images using the same method. All measurements **by a blinded investigator** were repeated for three times to obtain a mean.

Western blot analysis

CSF samples were used for Western blot to detect the expression of HO-1 and activation of complement (C5b-9 and C3a). Western blots were performed according to standard protocols (28). Briefly, 15μl CSF was loaded and separated by SDS-polyacrylamide gel electrophoresis (SDS-PAGE) and transferred to nitrocellulose membrane (Amersham, NJ, USA). Membranes were blocked with 5% nonfat milk and incubated in primary antibodies (rabbit anti-rat HO-1, 1:2000 dilution, StressGen; mouse anti- rat C5b-9 and chicken anti-rat C3a, 1:1000 dilution, Abcam) and secondary antibodies. Then membranes were developed by ECL chemiluminescence system (Amersham, NJ, USA) and exposed to films. Band densities were analyzed by IMAGE-J software.

NIH-PA Author Manuscript

NIH-PA Author Manuscript

NIH-PA Author Manuscript

Hematoxylin and Eosin staining

Twelve μm thick brain sections were stained with hematoxylin and eosin to examine morphology. Briefly, after washing in PBS (0.01mol/L, pH 7.4), sections were stained in Gill's hematoxylin solution (Sigma-Aldrich, MO, USA) for 5 seconds, and washed under running tap water for 5 minutes. Then sections were differentiated in 1% acid alcohol and blued in 0.2% ammonia water solution, followed by counterstaining with 0.5% eosin (Sigma-Aldrich, MO, USA) for 4 minutes, washed off, dehydrated in progressive alcohol concentrations, cleared in xylene, and mounted with Permount (Fisher Scientific, NJ, USA).

Immunohistochemistry

Acidin-biotin complex technique was applied for immunohistochemical staining according as described previously(29, 30). Brain slices (12μm thickness) were permeabilized with 0.3% triton X-100, blocked with 10% serum, and incubated overnight with primary antibodies (rabbit anti-rat HO-1, 1:400 dilution, StressGen; mouse anti-rat C5b-9 and chicken anti-rat C3a, 1:200 dilution, Abcam). Endogenous peroxidase activity was quenched by incubation in 0.3% hydrogen peroxide/methanol solution for 20 minutes, and followed by biotinylated secondary antibody and AB enzyme reagent for 1 hour, respectively. Diaminobenzidine (DAB) was used as the chromogen. Sections incubated in the absence of primary antibodies were used as negative controls.

Tissue and CSF hemoglobin concentrations

Tissue hemoglobin levels were determined by QuantiChrom Hemoglobin Assay Kit (BioAssay Systems, CA, USA) as described previously (31). Briefly, intravascular hemoglobin contamination was removed by intracardiac perfusion with 0.1M PBS under lethal anesthesia. Brains were weighed, homogenized in PBS (0.1M, pH 7.4), and centrifuged (13,000×g, 30 min). Then 50μl of supernatant was mixed with 200μl reagent for 5 min before reading at 400nm wavelength with a spectrophotometer. Hemoglobin concentration in brain tissue was expressed as mg/g.

CSF hemoglobin was measured using a commercial enzyme-linked immunosorbent assay (rat hemoglobin ELISA, Kamiya Biomedical, WA, USA). CSF samples were collected by cisterna magna puncture under deep anesthesia. Briefly, after adding 100μl diluted samples into anti-hemoglobin antibody pre-coated wells, the plate was incubated for 1 hour at room temperature, followed by four washes. Then, anti-hemoglobin antibody conjugated with horseradish peroxidase (HRP) was added. After incubation for 30 min and washing four times, tetramethylbenzidine, as a chromogenic substrate, was added to the formed HRP-complex to develop color for 10 min. The reaction was terminated by stop solution and the plate was read at 450nm wavelength on a microplate reader (BioTek, VT, USA). The amount of hemoglobin in each CSF sample calculated from a standard curve and expressed as ng/ml.

NIH-PA Author Manuscript

NIH-PA Author Manuscript

NIH-PA Author Manuscript

Statistical analysis

Statistical analyses were performed with KaleidaGraph (Version 4.0). All data are expressed as mean ± SE. Statistical comparisons were assessed by one-way ANOVA with Student Newman Keuls *post-hoc* tests. Statistical significance was set at $p<0.05$.

Results

Percussion injury parameters, mortality, and general physiological parameters

There was no significant difference in the recorded fluid percussion pressures between TBI and TBI+DFX groups (2.69 ± 0.13 vs. 3.00 ± 0.25 atm). Total mortality after TBI was 19.4% (13/67, including both TBI and TBI+DFX groups), **with most mortality (11/13) occurring immediately after TBI because of respiratory failure**. All recorded physiological parameters including hematocrit (Hct), mean arterial blood pressure (mBP), blood pH, PaO_2, $PaCO_2$, blood glucose, except the body weight loss, were controlled within normal ranges. There was a greater body weight loss in the TBI group (14.1 ± 3.0% of initial) than in sham-operated rats (2.2 ± 0.6%, $p<0.05$), but it was similar to that in the DFX-treated group (10.3 ± 1.0%, $p>0.05$).

Hemorrhagic lesions caused by TBI

Histology and T2* MRI were used to detect hemorrhagic lesions after TBI. Such lesions were found in and around the ipsilateral corpus callosum, and intraventricular and periventricular areas. In addition, some rats showed superficial hemorrhage on the brain ventral side. We also found subdural, subarachnoid hemorrhage and superficial cortical hemorrhage when the skull was opened after euthanasia. Hemorrhagic lesions on T2* images coincided with those in H&E stained brain sections (Fig.1).

Hydrocephalus induced by TBI

Ventricle volumes were measured on T2 MRI images. Representative T2 images at the levels of the lateral ventricle, aqueduct and fourth ventricle are shown in Fig.2. **TBI resulted in lateral ventricle dilation (24.1 ± 3.0 mm^3 vs. 9.9 ± 0.2 mm^3 in sham group, $p<0.05$)**. The aqueduct and fourth ventricles were slightly dilated after TBI. In a review of all slices, there were no blood clots in the connections between different ventricles (including the foramen of Monro and aqueduct) and no obvious ventricular compression resulting from brain edema.

Hydrocephalus following intraventricular injection of iron

To evaluate the effect of iron on ventricular dilation, rats received an injection of either 200μl $FeCl_3$ or saline into the right lateral ventricle. At 24 hours after injection, T2 MRI demonstrated significant bilateral ventricular enlargement in the $FeCl_3$ injected group (25.7 ± 3.4 mm^3) compared to saline injected rats (9.0 ± 0.6 mm^3, $p<0.01$, Fig.3).

DFX treatment attenuated TBI-induced hydrocephalus

Treatment with DFX (100mg/kg), at 2 and 14 hours after TBI, resulted in smaller lateral ventricular volume compared with vehicle-treated rats (Fig.4A). DFX treatment reduced not

NIH-PA Author Manuscript

NIH-PA Author Manuscript

NIH-PA Author Manuscript

only ipsilateral ventricular volume (5.6 ± 0.9 mm^3 vs. 12.8 ± 1.2 mm^3 in vehicle-treated group, $p<0.01$), but also contralateral ventricular volume (4.7 ± 0.8 mm^3 vs. 11.3 ± 1.9 mm^3 in vehicle treated group, $p<0.01$ Fig.4B).

DFX reduced upregulation of HO-1, but not C5b-9 and C3a, after TBI

Western blotting and immunohistochemical staining were performed to detect the expression of HO-1 and two components of the complement pathway (C3a and C5b-9). TBI resulted in increased HO-1, C5b-9 and C3a immunoreactivity in the periventricular area (Fig.5A). TBI induced the upregulation of HO-1 levels in CSF, which was attenuated by DFX treatment ($p<0.01$, Fig.5B). Both C3a and C5b-9 levels in CSF were also increased after TBI but did not affect by DFX treatment (Fig.5C, D).

DFX did not reduced brain hemorrhage after TBI

TBI resulted in higher hemoglobin concentrations in the ipsilateral hemisphere (1.11 ± 0.15 vs. 0.49 ± 0.02 mg/g in sham group, $p<0.01$) and CSF (328 ± 19 vs. 2.5 ± 1.2 ng/ml in sham group, $p<0.01$) (Fig.6A, B). Brain and CSF hemoglobin levels were not significantly reduced by DFX treatment (Fig.6A, B). T2* lesion size also did not differ between DFX- and the vehicle-treated groups ($p>0.05$, Fig. 6C).

Discussion

The major findings of the present study are: (1) intraparenchymal hematomas were present in the lateral fluid-percussion-induced TBI model, which were mainly located in and around the ipsilateral corpus callosum and the periventricular area; (2) acute ventricular dilation occurred by 24 hours after TBI; (3) intraventricular injection of iron also resulted in lateral ventricular enlargement; (4) DFX treatment attenuated TBI-induced ventricular enlargement and upregulation of HO-1; and (5) DFX did not affect CSF complement components (C3a, C5b-9) levels and hemorrhagic lesion volume after TBI.

Lateral fluid percussion devices have been used to induce TBI since the 1980s. Previous studies have produced detailed information about the physiological, histopathological and neurological changes of TBI (32-34). In almost all experimental animals, hemorrhage is found in multiple locations, including subdual, subarachnoid and intraparenchymal (mostly within white/gray matter interface, corpus callosum, hippocampus, ventricles and periventricular area). Similar results were found in the current study. Intraparenchymal hemorrhage is almost always restricted to ipsilateral hemisphere in lateral fluid percussion model, while bilateral hemorrhage mostly occurs in TBI induced by midline fluid percussion.

Extravascular erythrocytes may lyse via activation of complement cascade and formation of membrane attack complex (MAC) (35, 36), and we found enhanced expression of C3a and C5b-9 in the periventricular area and CSF after TBI. Heme, derived from released hemoglobin, is degraded into iron, carbon monoxide, and biliverdin (which is then converted into bilirubin) by heme oxygenases (HOs). Injection of hemoglobin into subarachnoid space can stimulate HO-1 expression in all brain regions at 24 hours (37). HOs, by accelerating

NIH-PA Author Manuscript

NIH-PA Author Manuscript

NIH-PA Author Manuscript

heme metabolism, may contribute to brain iron overload. This study showed upregulation of CSF HO-1 protein levels and increased periventricular HO-1 immunoreactivity.

Ventriculomegaly is a frequent phenomenon after severe head injury, and is observed as early as 7 hours after ictus (38). Almost 44% of severe head injury survivors developed ventriculomegaly, and half of them were diagnosed as PTH according to CSF dynamic characterizations (3). Post-traumatic hydrocephalus has been well-recognized in TBI survival patients. CT and MRI are the two most commonly used methods for diagnosis of PTH (39), and MRI is becoming more popular in clinical use because of high image quality, three-dimensional images, examination of CSF flow dynamics and lack of radiation exposure, especially for pediatric patients. In this study, T2-weighted MRI was performed for the detection of ventricular enlargement after TBI, and it showed almost 100% rats developed ventriculomegaly. **However, a limitation of this study is the lack of a baseline MRI and the small number of animals in the sham group.**

A T2* sequence was used as a sensitive method to detect hyperacute and subacute hemorrhage (e.g. ICH). In ICH, T2* sequence could detect the lesion in both experimental animal models and clinical patients within 30 minutes post-ictus (40, 41). When using T2* MR scanning in long-term survivors of ICH or IVH, researchers found the hypointensive lesions in and around the hematoma(19). The hypointensity in T2* images was due to the iron accumulation, which has susceptibility effects to reduce T2 relaxation time (42). Our previous study in ICH also indicated that T2* lesions coincide with the histological distribution of hematomas and iron deposition after ICH(19).

A number of studies have examined the mechanisms of early ventriculomegaly. It may be due to mechanical obstruction of CSF flow pathways (43, 44). In acute post-hemorrhagic hydrocephalus, erythrocytes were found accumulating and degenerating in arachnoid villi (45). The role of erythrocyte components in CSF, such as iron, in the development of ventricular enlargement and hydrocephalus has less studied. However, previous research has provided several pieces of evidence supporting the importance of iron in hydrocephalus development. One study from Iwanowski and his colleague in 1960 was the first report on iron-related hydrocephalus (46). They injected Imferon (iron-dextran complex) or blood into the cisterna magna of dogs, and found hydrocephalus and iron deposition were the common pathological changes in all animals. In the two animals receiving Imferon injection (3 times per week), hydrocephalus was noted at days 24 and 30 when the animals were sacrificed. In patients, concentrations of iron and ferritin (an endogenous iron chelator) are increased markedly in CSF after SAH and remain at high levels for 2 weeks (16). SAH is a common cause of hydrocephalus, and CSF ferritin levels, but not non-heme iron levels measured 3-14 days after ictus, were significantly elevated in SAH patients with hydrocephalus (47). The importance of CSF iron homeostasis is also reflected by the high expression of proteins involved in iron regulation at the choroid plexus, including transferrin receptor, DMT1 and ceruloplasmin (48, 49).

Further evidence of a potential role of iron in acute ventriculomegaly after TBI is found in the current study: (a) SAH, IVH and markedly increased CSF hemoglobin were found after lateral fluid percussion-induced TBI; (b) complement activation and the upregulation of

NIH-PA Author Manuscript

NIH-PA Author Manuscript

NIH-PA Author Manuscript

HO-1 in CSF indicate potentially enhanced erythrocyte lysis and heme metabolism after TBI, which could produce several degradation products, including Fe^{3}+; (c) intraventricular injection of $FeCl_3$ resulted in acute ventricular dilation at 24 hours, which was a strong proof of the participation of iron in the acute ventricular dilation; (d) DFX, an iron chelator, attenuated TBI-induced acute ventricolomegaly. Future studies should examine the underlying mechanisms of iron in the development of acute ventricular dilation and hydrocephalus.

DFX has been used clinically for the treatment of acute and chronic iron overload since 1960's. DFX stably binds ferric ions via its three hydroxamic acid groups. DFX can bind and remove iron from ferritin and hemosiderin in a concentration-dependent manner (50). DFX may remove about 10-15% iron from saturated transferrin, but none from hemoglobin (50). Studies have shown that DFX reduces brain injury and improves functional outcome in TBI models (20, 21). Our previous studies have also found that DFX can reduce iron levels in CSF after ICH, and attenuate ventricular enlargement following IVH (15, 24). Here we found a therapeutic effect of DFX in acute post-traumatic ventriculomegaly without affecting the initial injury (no difference in T2 lesion size or brain/CSF hemoglobin levels).

In summary, TBI caused brain hemorrhage and acute hydrocephalus in this rat lateral fluid percussion model. Intraventricular injection of iron also resulted in hydrocephalus and DFX treatment abolished TBI-induced hydrocephalus. These results suggest a role of iron in hydrocephalus development after TBI.

Acknowledgments

Sources of Funding: This study was supported by grants NS-073595, NS-079157 and NS-084049 from the National Institutes of Health (NIH). The content is solely the responsibility of the authors and does not necessarily represent the official view of the NIH.

References

1. Langlois JA, Kegler SR, Butler JA, Gotsch KE, Johnson RL, Reichard AA, et al. Traumatic brain injury-related hospital discharges. Results from a 14-state surveillance system, 1997. MMWR Surveill Summ. 2003 Jun 27; 52(4):1–20. Epub 2003/07/03. eng. [PubMed: 12836629]
2. Faul, M. Traumatic brain injury in the United States : emergency department visits, hospitalizations, and deaths, 2002-2006. US Dept of Health and Human Services, Centers for Disease Control and Prevention, National Center for Injury Prevention and Control; 2010.
3. Marmarou A, Foda MA, Bandoh K, Yoshihara M, Yamamoto T, Tsuji O, et al. Posttraumatic ventriculomegaly: hydrocephalus or atrophy? A new approach for diagnosis using CSF dynamics. J Neurosurg. 1996 Dec; 85(6):1026–35. Epub 1996/12/01. eng. [PubMed: 8929491]
4. Cardoso ER, Galbraith S. Posttraumatic hydrocephalus--a retrospective review. Surgical neurology. 1985; 23:261–4. [PubMed: 3975808]
5. Hawkins TD, Lloyd AD, Fletcher GI, Hanka R. Ventricular size following head injury: a clinico-radiological study. Clin Radiol. 1976 Jul; 27(3):279–89. Epub 1976/07/01. eng. [PubMed: 1086181]
6. Kishore PR, Lipper MH, Miller JD, Girevendulis AK, Becker DP, Vines FS. Post-traumatic hydrocephalus in patients with severe head injury. Neuroradiology. 1978; 16:261–5. Epub 1978/01/01. eng. [PubMed: 740188]
7. Chang EF, Meeker M, Holland MC. Acute traumatic intraparenchymal hemorrhage: risk factors for progression in the early post-injury period. Neurosurgery. 2006 Apr; 58(4):647–56. discussion -56. Epub 2006/04/01. eng. [PubMed: 16575328]

NIH-PA Author Manuscript

NIH-PA Author Manuscript

NIH-PA Author Manuscript

8. Maas AI, Stocchetti N, Bullock R. Moderate and severe traumatic brain injury in adults. Lancet Neurol. 2008 Aug; 7(8):728–41. Epub 2008/07/19. eng. [PubMed: 18635021]
9. Xu Y, McArthur DL, Alger JR, Etchepare M, Hovda DA, Glenn TC, et al. Early nonischemic oxidative metabolic dysfunction leads to chronic brain atrophy in traumatic brain injury. J Cereb Blood Flow Metab. 2010 Apr; 30(4):883–94. Epub 2009/12/24. eng. [PubMed: 20029449]
10. Xi G, Keep RF, Hoff JT. Mechanisms of brain injury after intracerebral haemorrhage. Lancet Neurol. 2006 Jan; 5(1):53–63. Epub 2005/12/20. eng. [PubMed: 16361023]
11. Nakamura T, Keep Richard F, Hua Y, Schallert T, Hoff Julian T, Xi G. Deferoxamine-induced attenuation of brain edema and neurological deficits in a rat model of intracerebral hemorrhage. Journal of neurosurgery. 2004; 100(4):672–8. [PubMed: 15070122]
12. Hua Y, Nakamura T, Keep RF, Wu J, Schallert T, Hoff JT, et al. Long-term effects of experimental intracerebral hemorrhage: the role of iron. J Neurosurg. 2006 Feb; 104(2):305–12. Epub 2006/03/03. eng. [PubMed: 16509506]
13. Chen B, Cheng Q, Yang K, Lyden PD. Thrombin mediates severe neurovascular injury during ischemia. Stroke; a journal of cerebral circulation. 2010 Oct; 41(10):2348–52. Epub 2010/08/14. eng. [PubMed: 20705928]
14. Kjellin KG. The CSF iron in patients with neurological diseases. Acta Neurol Scand. 1967; 43(3): 299–313. [PubMed: 4227818]
15. Wan S, Hua Y, Keep RF, Hoff JT, Xi G. Deferoxamine reduces CSF free iron levels following intracerebral hemorrhage. Acta neurochirurgica Supplement. 2006; 96:199–202. Epub 2006/05/05. eng. [PubMed: 16671454]
16. Suzuki H, Muramatsu M, Kojima T, Taki W. Intracranial heme metabolism and cerebral vasospasm after aneurysmal subarachnoid hemorrhage. Stroke. 2003 Dec; 34(12):2796–800. Epub 2003/12/06. eng. [PubMed: 14657544]
17. Onyszchuk G, LeVine SM, Brooks WM, Berman NEJ. Post-acute pathological changes in the thalamus and internal capsule in aged mice following controlled cortical impact injury: a magnetic resonance imaging, iron histochemical, and glial immunohistochemical study. Neuroscience letters. 2009; 452:204–8. [PubMed: 19383440]
18. Raz E, Jensen JH, Ge Y, Babb JS, Miles L, Reaume J, et al. Brain iron quantification in mild traumatic brain injury: a magnetic field correlation study. AJNR American journal of neuroradiology. 2011; 32:1851–6. [PubMed: 21885717]
19. Wu G, Xi G, Hua Y, Sagher O. T2* Magnetic Resonance Imaging Sequences Reflect Brain Tissue Iron Deposition Following Intracerebral Hemorrhage. Transl Stroke Res. 2010 Mar 1; 1(1):31–4. Epub 2010/09/03. Eng. [PubMed: 20811505]
20. Zhang L, Hu R, Li M, Li F, Meng H, Zhu G, et al. Deferoxamine attenuates iron-induced long-term neurotoxicity in rats with traumatic brain injury. Neurol Sci. 2013 May; 34(5):639–45. Epub 2012/04/28. eng. [PubMed: 22538758]
21. Long DA, Ghosh K, Moore AN, Dixon CE, Dash PK. Deferoxamine improves spatial memory performance following experimental brain injury in rats. Brain Res. 1996 Apr 22; 717(1-2):109–17. Epub 1996/04/22. eng. [PubMed: 8738260]
22. Okauchi M, Hua Y, Keep RF, Morgenstern LB, Schallert T, Xi G. Deferoxamine treatment for intracerebral hemorrhage in aged rats: therapeutic time window and optimal duration. Stroke. 2010 Feb; 41(2):375–82. Epub 2010/01/02. eng. [PubMed: 20044521]
23. Okauchi M, Hua Y, Keep RF, Morgenstern LB, Xi G. Effects of deferoxamine on intracerebral hemorrhage-induced brain injury in aged rats. Stroke. 2009 May; 40(5):1858–63. Epub 2009/03/17. eng. [PubMed: 19286595]
24. Chen Z, Gao C, Hua Y, Keep RF, Muraszko K, Xi G. Role of iron in brain injury after intraventricular hemorrhage. Stroke. 2010 Feb; 42(2):465–70. Epub 2010/12/18. eng. [PubMed: 21164132]
25. Lee JY, Keep RF, He Y, Sagher O, Hua Y, Xi G. Hemoglobin and iron handling in brain after subarachnoid hemorrhage and the effect of deferoxamine on early brain injury. J Cereb Blood Flow Metab. 2010 Nov; 30(11):1793–803. Epub 2010/08/26. eng. [PubMed: 20736956]

NIH-PA Author Manuscript

NIH-PA Author Manuscript

NIH-PA Author Manuscript

26. Dixon CE, Lighthall JW, Anderson TE. Physiologic, histopathologic, and cineradiographic characterization of a new fluid-percussion model of experimental brain injury in the rat. J Neurotrauma. 1988; 5(2):91–104. Epub 1988/01/01. eng. [PubMed: 3225860]
27. Kabadi SV, Hilton GD, Stoica Ba, Zapple DN, Faden AI. Fluid-percussion-induced traumatic brain injury model in rats. Nature protocols. 2010; 5:1552–63. [PubMed: 20725070]
28. Xi G, Keep RF, Hua Y, Xiang J, Hoff JT. Attenuation of thrombin-induced brain edema by cerebral thrombin preconditioning. Stroke. 1999 Jun; 30(6):1247–55. Epub 1999/06/04. eng. [PubMed: 10356108]
29. Jin H, Xi G, Keep RF, Wu J, Hua Y. DARPP-32 to quantify intracerebral hemorrhage-induced neuronal death in basal Ganglia. Transl Stroke Res. 2013 Feb; 4(1):130–4. [PubMed: 23543809]
30. Guo F, Hua Y, Wang J, Keep RF, Xi G. Inhibition of carbonic anhydrase reduces brain injury after intracerebral hemorrhage. Translational Stroke Research. 2012 Mar 1; 3(1):130–7. Epub 2012/03/09. Eng. [PubMed: 22400066]
31. Qin Z, Karabiyikoglu M, Hua Y, Silbergleit R, He Y, Keep RF, et al. Hyperbaric oxygen-induced attenuation of hemorrhagic transformation after experimental focal transient cerebral ischemia. Stroke. 2007 Apr; 38(4):1362–7. Epub 2007/02/27. eng. [PubMed: 17322079]
32. Dixon CE, Lyeth BG, Povlishock JT, Findling RL, Hamm RJ, Marmarou A, et al. A fluid percussion model of experimental brain injury in the rat. J Neurosurg. 1987 Jul; 67(1):110–9. Epub 1987/07/01. eng. [PubMed: 3598659]
33. McIntosh TK, Noble L, Andrews B, Faden AI. Traumatic brain injury in the rat: characterization of a midline fluid-percussion model. Cent Nerv Syst Trauma. 1987; 4(2):119–34. Epub 1987/01/01. eng. [PubMed: 3690695]
34. McIntosh TK, Vink R, Noble L, Yamakami I, Fernyak S, Soares H, et al. Traumatic brain injury in the rat: characterization of a lateral fluid-percussion model. Neuroscience. 1989; 28(1):233–44. Epub 1989/01/01. eng. [PubMed: 2761692]
35. Hua Y, Xi G, Keep RF, Hoff JT. Complement activation in the brain after experimental intracerebral hemorrhage. J Neurosurg. 2000; 92(6):1016–22. [PubMed: 10839264]
36. Bellander BM, Singhrao SK, Ohlsson M, Mattsson P, Svensson M. Complement activation in the human brain after traumatic head injury. Journal of Neurotrauma. 2001; 18(12):1295–311. [PubMed: 11780861]
37. Turner CP, Bergeron M, Matz P, Zegna A, Noble LJ, Panter SS, et al. Heme oxygenase-1 is induced in glia throughout brain by subarachnoid hemoglobin. Journal of Cerebral Blood Flow & Metabolism. 1998; 18(3):257–73. [PubMed: 9498842]
38. Takagi H, Tamaki Y, Morii S, Ohwada T. Rapid enlargement of ventricles within seven hours after head injury. Surgical neurology. 1981; 16:103–5. [PubMed: 7280980]
39. Losowska-Kaniewska D, Oles A. Imaging examinations in children with hydrocephalus. Adv Med Sci. 2007; 52(Suppl 1):176–9. Epub 2008/01/31. eng. [PubMed: 18229659]
40. Kuker W, Thiex R, Rohde I, Rohde V, Thron A. Experimental acute intracerebral hemorrhage. Value of MR sequences for a safe diagnosis at 1.5 and 0.5 T. Acta Radiol. 2000 Nov; 41(6):544–52. Epub 2000/11/25. eng. [PubMed: 11092473]
41. Linfante I, Llinas RH, Caplan LR, Warach S. MRI features of intracerebral hemorrhage within 2 hours from symptom onset. Stroke. 1999 Nov; 30(11):2263–7. Epub 1999/11/05. eng. [PubMed: 10548654]
42. de Backer ME, Nabuurs RJ, van Buchem MA, van der Weerd L. MR-based molecular imaging of the brain: the next frontier. AJNR Am J Neuroradiol. 2010 Oct; 31(9):1577–83. Epub 2010/09/25. eng. [PubMed: 20864520]
43. Nahed BV, Darbar A, Doiron R, Saad A, Robson CD, Smith ER. Acute hydrocephalus secondary to obstruction of the foramen of monro and cerebral aqueduct caused by a choroid plexus cyst in the lateral ventricle. Case report. J Neurosurg. 2007 Sep; 107(3 Suppl):236–9. Epub 2007/10/09. eng. [PubMed: 17918533]
44. Yoshimoto Y, Ochiai C, Kawamata K, Endo M, Nagai M. Aqueductal blood clot as a cause of acute hydrocephalus in subarachnoid hemorrhage. AJNR Am J Neuroradiol. 1996 Jun-Jul;17(6): 1183–6. Epub 1996/06/01. eng. [PubMed: 8791935]

NIH-PA Author Manuscript

NIH-PA Author Manuscript

NIH-PA Author Manuscript

45. Massicotte EM, Del Bigio MR. Human arachnoid villi response to subarachnoid hemorrhage: possible relationship to chronic hydrocephalus. J Neurosurg. 1999 Jul; 91(1):80–4. Epub 1999/07/02. eng. [PubMed: 10389884]

46. Iwanowski L, Olszewski J. The effects of subarachnoid injections of iron-containing substances on the central nervous system. J Neuropathol Exp Neurol. 1960 Jul.19:433–48. Epub 1960/07/01. eng. [PubMed: 14406175]

47. Suzuki H, Muramatsu M, Tanaka K, Fujiwara H, Kojima T, Taki W. Cerebrospinal fluid ferritin in chronic hydrocephalus after aneurysmal subarachnoid hemorrhage. Journal of neurology. 2006; 253:1170–6. [PubMed: 16649098]

48. Rouault TA, Zhang DL, Jeong SY. Brain iron homeostasis, the choroid plexus, and localization of iron transport proteins. Metab Brain Dis. 2009 Dec; 24(4):673–84. Epub 2009/10/24. eng. [PubMed: 19851851]

49. Moos T, Morgan EH. Transferrin and transferrin receptor function in brain barrier systems. Cell Mol Neurobiol. 2000 Feb; 20(1):77–95. Epub 2000/02/26. eng. [PubMed: 10690503]

50. Keberle H. The Biochemistry of Desferrioxamine and Its Relation to Iron Metabolism. Ann N Y Acad Sci. 1964 Oct 7.119:758–68. Epub 1964/10/07. eng. [PubMed: 14219455]

NIH-PA Author Manuscript
NIH-PA Author Manuscript
NIH-PA Author Manuscript

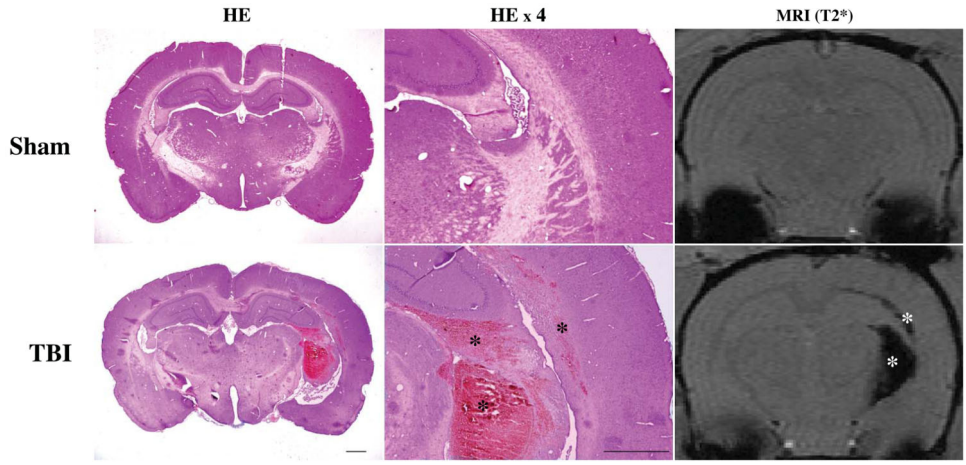

Figure 1.

Representative coronal brain sections with H&E staining and T2* gradient-echo sequence images from a rat 24 hours after a sham operation and another rat 24 hours after TBI. Note that areas with hemorrhagic lesions (asterisks) are noticeable after TBI with both H&E staining and T2* imaging and that there is congruence between the two imaging parameters. Scale bars =1 mm.

NIH-PA Author Manuscript

NIH-PA Author Manuscript

NIH-PA Author Manuscript

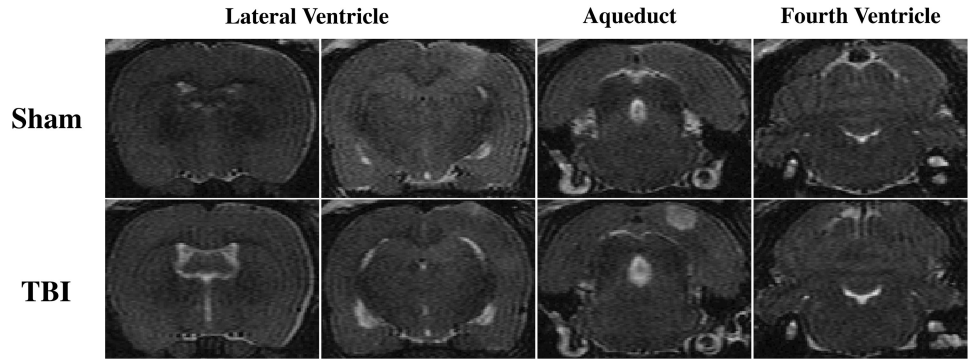

Figure 2.

Representative T2-weighted coronal images at the level of the lateral ventricles (∼0.6 and 3.7 mm posterior to bregma), aqueduct and fourth ventricle (∼8.6 mm posterior to bregma) 24 hours after sham operation or TBI.

NIH-PA Author Manuscript

NIH-PA Author Manuscript

NIH-PA Author Manuscript

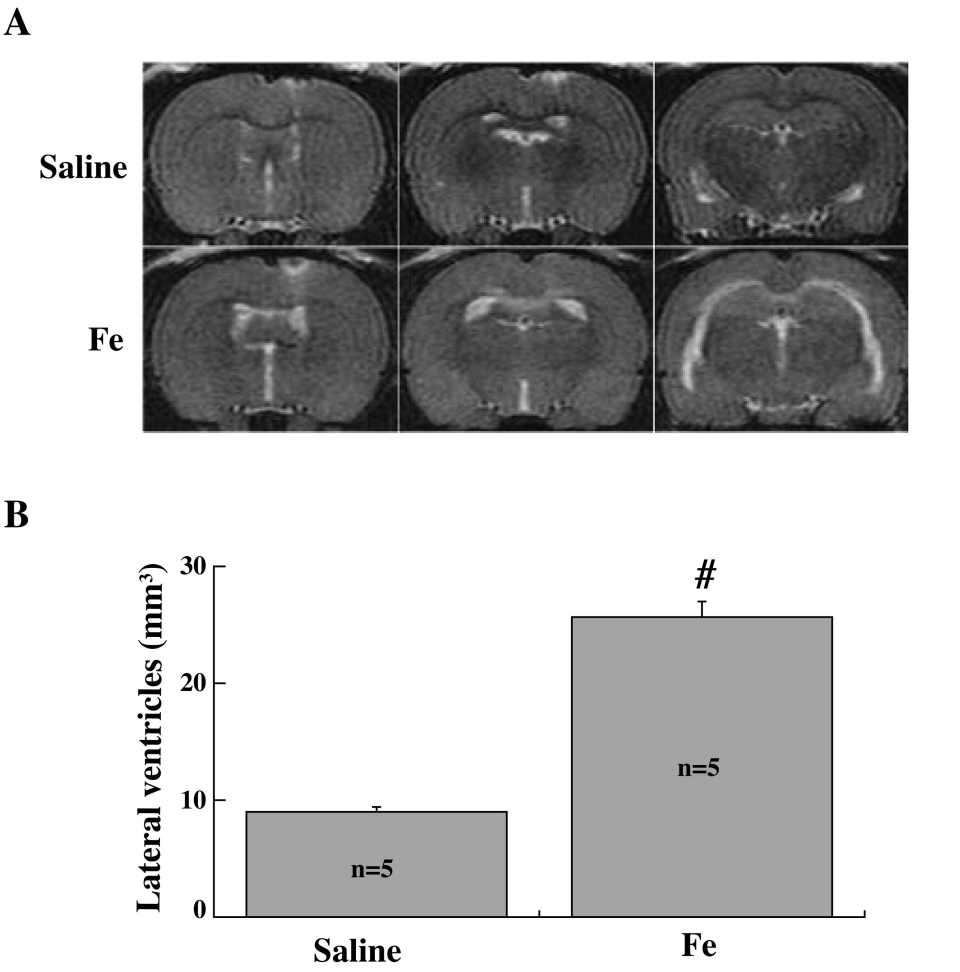

Figure 3.

T2 images (**A**) and lateral ventricle volume measurements (**B**) in rats injected with either 200μl $FeCl_3$ (0.5 mmol/L, n=5) or saline (n=5) into the right lateral ventricle. Measurements are at 24 hours after the injection. Values are mean ± SE, # $p<0.01$ vs. saline group, n=5 per group.

NIH-PA Author Manuscript

NIH-PA Author Manuscript

NIH-PA Author Manuscript

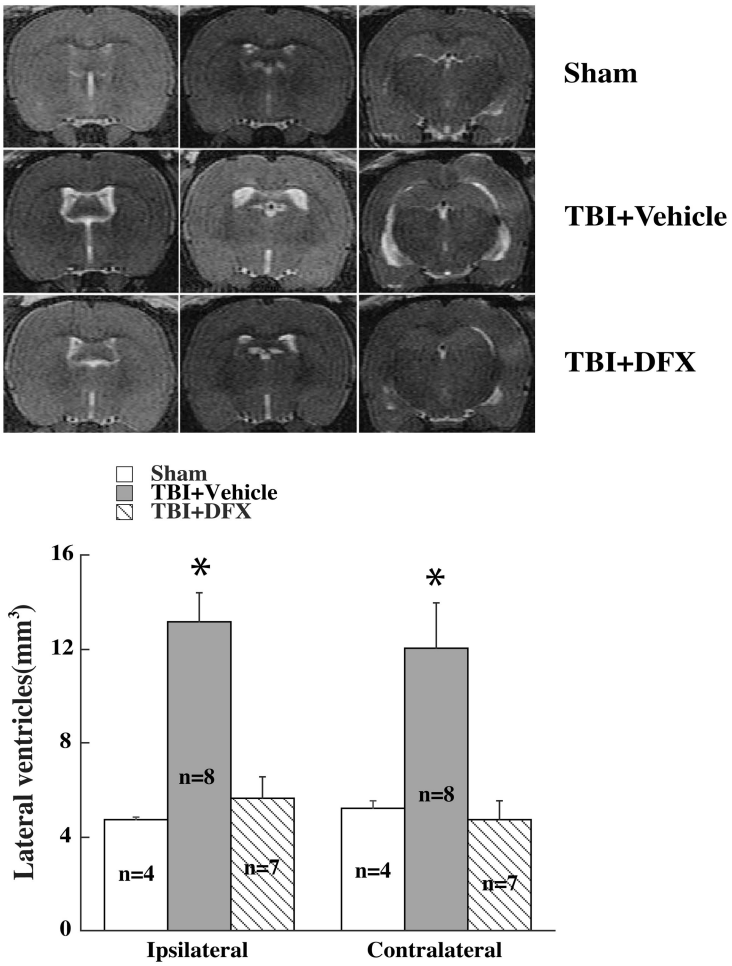

Figure 4.

T2 imaging and lateral ventricle volume measurements at 24 hours in rats undergoing sham-operation or TBI. TBI animals were treated with deferoxamine (DFX, 100 mg/kg, or vehicle at 2 and 14 hours after TBI). Values are mean ± SE, * $p<0.05$ vs. sham or TBI+DFX group.

NIH-PA Author Manuscript
NIH-PA Author Manuscript
NIH-PA Author Manuscript

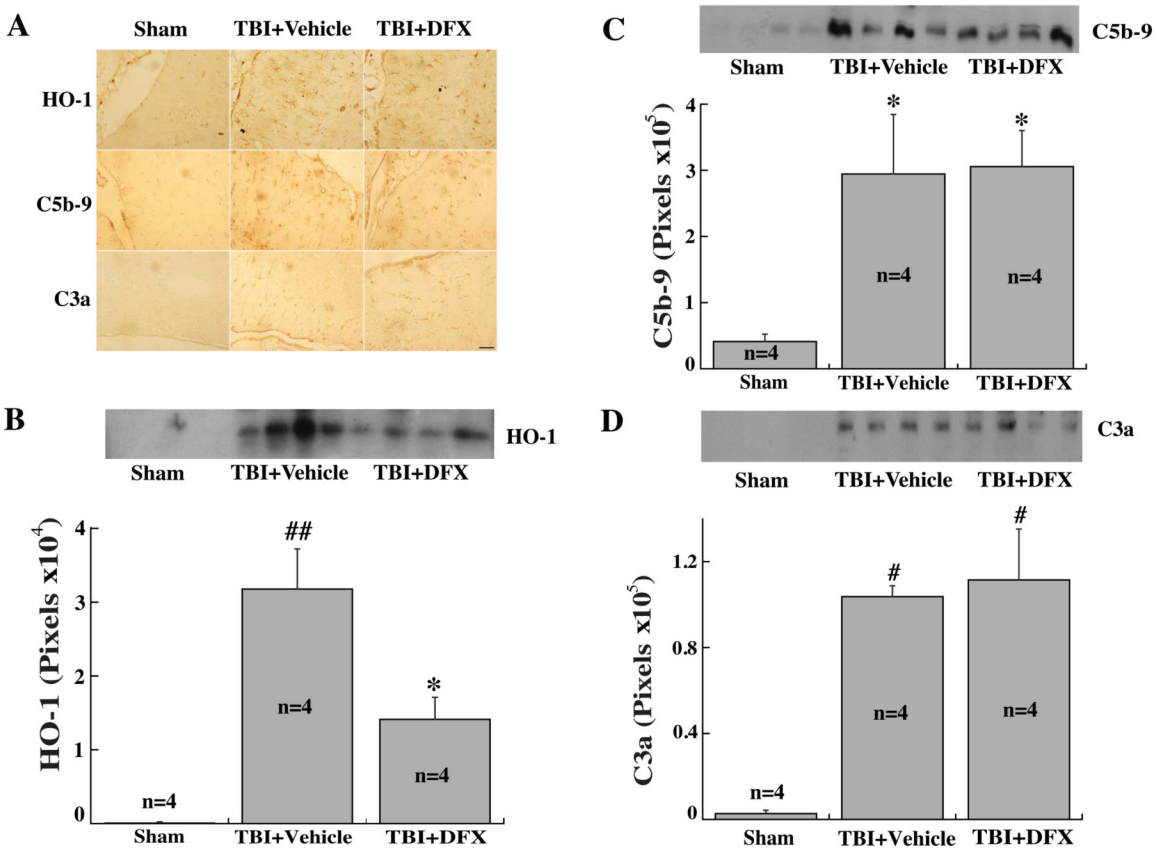

Figure 5.

(**A**) The immunoreactivity of heme oxygenase-1 (HO-1), and complement C5b-9 and C3a in the ipsilateral periventricular area 24 hours after sham-operation or TBI with or without DFX treatment. Scale bar=50μm. (**B**) HO-1, (**C**) C5b-9 and (**D**) C3a protein levels in the CSF at 24 hours after sham-operation or TBI with or without DFX treatment. Values are mean ± SE, n=4 for each group, * $p<0.05$, # $p<0.01$ vs. sham group. ## $p<0.01$ vs. the other groups.

NIH-PA Author Manuscript

NIH-PA Author Manuscript

NIH-PA Author Manuscript

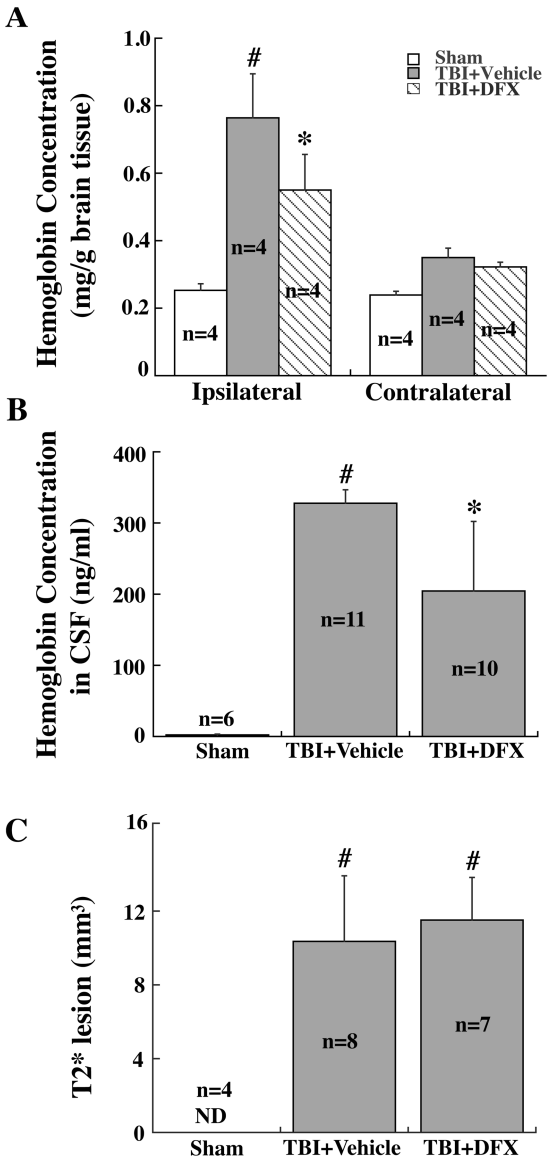

Figure 6.

Hemoglobin concentrations in the hemisphere (**A**) and CSF (**B**), and T2* lesion volumes (**C**) in rats that had sham operation or TBI with or without DFX treatment at 24 hours. Values are means ± SE, n=4-11; * $p<0.05$, # $p<0.01$ vs. Sham group. ND = not detected.